

Quantification of digital image correlation applicability related to in-situ proof load testing of bridges

Christian Overgaard Christensen¹, Eva O.L. Lantsoght^{2,3}, Jacob Wittrup Schmidt¹

¹ Department of Civil Engineering, Technical University of Denmark, Kgs. Lyngby, Denmark

² Politécnico, Universidad San Francisco de Quito, Quito, Ecuador

³ Concrete Structures, Department of Engineering Structures, Delft University of Technology, Delft, the Netherlands

Contact e-mail: coch@byg.dtu.dk

ABSTRACT: Advanced crack monitoring is crucial for high precision response- and threshold evaluation when performing proof- and diagnostic load tests on existing concrete structures. Mostly, crack monitoring techniques involve one monitoring method, which provide thresholds with regard to stop criteria and characterization information. In the ongoing Danish bridge testing research program, it is hypothesized that several independent monitoring techniques are needed to reduce uncertainties related to crack detection and categorization. A number of novel monitoring methods are used in the research project. A special focus is however dedicated to two-dimensional digital image correlation (2D-DIC) and acoustic emission (AE). This paper presents initial research concerning evaluations related to digital image correlation based on sub-component beam tests performed in the DTU CasMat laboratory facility. The tested beams were prefabricated as TT-elements with a length of 6.4 m and cut into two T-beam elements. The test matrix consisted of ten beams strengthened with carbon fiber reinforced polymer (CFRP) in different configurations with and without post-tensioning of the CFRP, thus resulting in different crack initiation behavior. The investigations in this paper include: (1) time of crack detection compared to visual detection, (2) time of crack detection compared to time of crack width threshold values, and (3) crack width evaluation using 2D-DIC strain correction for out-of-plane deflection. The results show that cracks can be detected prior to both visual detection and significant stiffness change. After detection, crack development can be monitored for crack width stop criteria. Crack widths can also be successfully monitored for surfaces subjected to out-of-plane movement using a geometric correction method. The methodology is hypothesized to be of significant importance in future testing of full-scale concrete slab bridges in the Danish bridge testing project.

1 INTRODUCTION

Recent decades have shown an increasing need for capacity evaluation of existing bridges. A mean to this is to perform full-scale tests to demonstrate the bridge capacity level and behavior. Some of the first full-scale proof loadings were performed in the early 1910s and many different types of bridge tests have been performed since then. In one of the earliest tests by Elmont (1913), a flat arch bridge was loaded by pieces of steel placed on the bridge. Later it was seen how hydraulic jacks could be used for loading by Rösli (1963). Another loading setup was demonstrated to simulate wheel pressures (Goodpasture and Burdette (1973)). More recent examples of bridge tests on short span concrete slab bridges have resulted in several studies on



the subject, (Zhang et al (2011, 2013); Schmidt et al (2014); Lantsoght et al (2016)). However, often it seems difficult to compare the performed bridge tests since the scopes, theoretical approaches, test procedures, and final outputs vary significantly.

1.1 Danish Research Project

In 2016, an ambitious research project concerning full-scale load testing and systematic reclassification of bridges was initiated in Denmark. So far, several single-span bridges have been tested using a novel test rig. For two of the tested OT-slab bridges (overturned T-beams with in-situ concrete cast on top), the results include output from separately controlled hydraulic jacks and several different sources of deformation measurements (surveyor, linear variable displacement transducers (LVDTs), distance lasers, and digital image correlation (DIC)), (Halding et al (2017); Schmidt et al (2018)).

1.2 Stop criteria

Stop criteria are a necessity when performing a non-destructive proof load test to make sure that the test does not cause irreversible damage to the bridge. Several countries have national guidelines for diagnostic and proof load testing (ICE (1998); DAfStb (2000); AASHTO (2011); ACI Committee 437 (2013); NRA (2014)), but only few present stop criteria (DAfStb (2000); ACI Committee 437 (2013)) for buildings and to the authors' knowledge none of them present fulfilling stop criteria for bridges. Evaluation of bridges can be difficult and the procedure for defining stop criteria is still up to discussion. Due to the complexity of a bridge structure, the bridge behavior might differ from the expected. Stop criteria should therefore be evaluated to an extent, where the criteria work independent of the bridge behavior. This might involve having multiple criteria to check for, from several independent monitoring sources, for different possible failure modes, and several bridge members or components that may be critical during the load test.

In 2018, a proposal for multiple stop criteria in proof load testing of reinforced concrete slab bridges was presented by Lantsoght et al (2018). The proposal follows the work in previous publications, (Lantsoght et al (2016, 2017)) and provides a solid base for further development. Criteria for both bending and shear failure are proposed, although the criteria for shear need further investigation. Eurocode 2 presents recommendations for service limit loads, which may be comparable to the described stop criteria, European Committee for Standardization (2008).

In addition to the presented stop criteria, an alternative stop criterion could be crack detection, which precedes crack width criteria. Crack detection as a stop criterion also has need for quantification of two parameters: (1) The probability of detection of a crack and (2) the probability that the detected actually is a crack and not a false positive.

1.3 Monitoring

Monitoring plays an essential role in proof load testing of bridges in terms of evaluating stop criteria. A large variety of monitoring equipment exists, which can monitor for the stop criteria described e.g. by Lantsoght et al (2018). To limit the amount of data sources and associated preparation time, the Danish bridge testing project primarily focusses on application of non-contact measurements and/or full-field monitoring. Two of the most promising methods are digital image correlation (DIC) and acoustic emissions (AE). It is hypothesized that the combined use of the two methods may provide the monitoring basis needed for robust stop criteria during proof load testing. The combined use is seen successfully applied by Omondi et al (2016), where pre-stressed railway sleepers are tested.

The project focusses on 2D DIC because of its quick and simple setup. 3D DIC often requires cumbersome preparation and calibration, which is not possible within the test time window.

Generally, it also offers a lower resolution than what is possible with 2D DIC. A high resolution is essential when monitoring large surfaces, such as the bottom surface of bridge slabs. The use of 2D DIC does however also present some challenges with regard to strain and crack width monitoring. The most significant challenges concern the out-of-plane movement and rotation of the surface that occur during testing. These effects are addressed by Halding et al (2018a) and Halding et al (2018b) where geometrical corrections are proposed.

In this paper the applicability of 2D DIC in evaluation of stop criteria is evaluated. Investigations are made regarding initial crack detection, crack width monitoring, and crack width correction for out-of-plane movement and rotation.

1.4 Geometric correction

Geometric corrections have to be considered to enable strain measurement evaluation using 2D DIC encountering out-of-plane movement. The full correction method corrects for two geometrical phenomena. The first correction is solely based on out-of-plane movement, where no surface rotation occurs. Given that the object moves closer, it will appear larger, which the DIC system interprets as a change in strain, Halding et al (2018a). The second component accounts for surface rotations by correcting for the object surface experiencing an angle change, Halding et al (2018b). Compared to the actual strain, the geometrical corrections are of significant magnitude. For the method to work as intended it is necessary to have very accurate data related to the surface deflection. If full deflection data is not available, the correction will mainly be applicable across mid-span, where no surface rotation occurs.

2 TEST AND MONITORING SETUP

The test beams used for the investigations in this paper were tested as part of a project concerning strengthening of existing structures using a carbon fiber reinforced polymer (CFRP) post-tensioning system. The tests included post tensioning to different levels and are therefore deemed to provide differences between the crack patterns of each test configuration.

2.1 Test beams

The full test series consisted of 7 T-section beams strengthened using the CFRP post-tensioning system. The beams had a length of 6.4 m and the cross section shown in Figure 1. All beams were tested in four point bending with a deformation controlled load rate of 2 mm/min. The support distance was 5 m and the load distributing beam had a span of 1.4 m, see Figure 2.

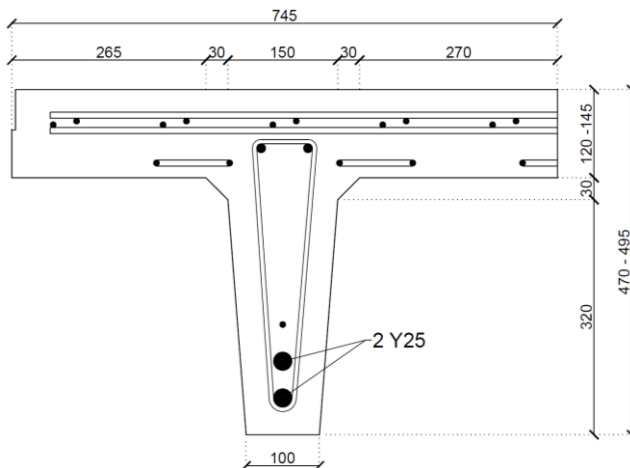


Figure 1. T-beam cross section. Units: mm.

Of the strengthened beams, two were strengthened with conventional near surface mounted reinforcement (NSMR) CFRP without post-tensioning and anchoring, and five were strengthened with the anchored post-tensioning system, where three were post-tensioned to 50 % of the CFRP manufacturers recommended ultimate capacity (approximately 1100 MPa) and two were post-tensioned to 70 % of the CFRP manufacturer strength (approximately 1550 MPa). They were cut longitudinally from precast TT-elements into single T-beams.

2.2 Monitoring setup

The beams were monitored using standard measurement equipment such as LVDTs and strain gauges, and for seven of the beams by DIC on the side of the beam web and from underneath as seen on Figure 2. A Canon 6D with 20 Mpx (Megapixel) resolution camera with a wide-angle lens (Canon EF 16-35mm f/2.8L II USM) was used from underneath and a Canon 750D with 24 Mpx resolution camera and a regular lens (Canon EFS 18-55mm IS STM) was used from the side. A pattern was painted on the concrete surface for better DIC detection but the laboratory conditions were not altered with artificial lighting.

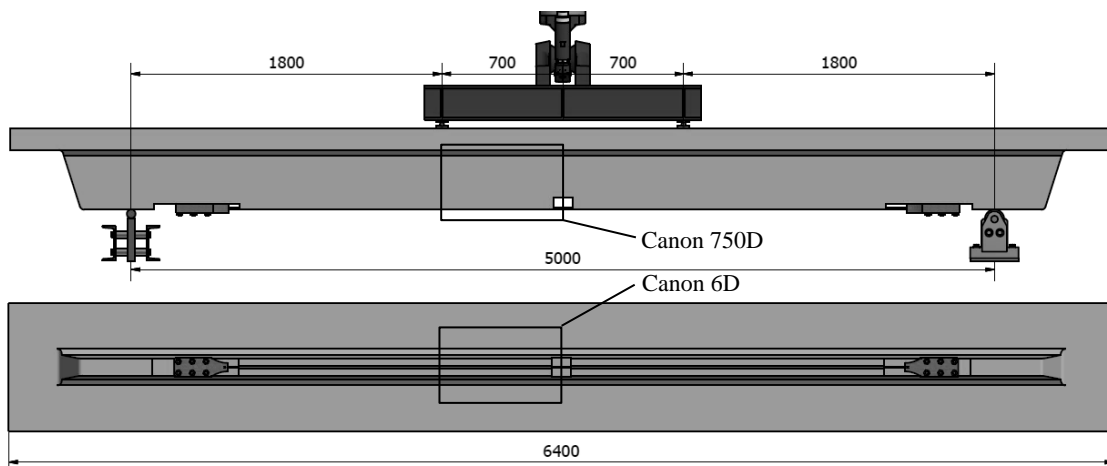


Figure 2. Test beam and DIC setup. Units: mm.

3 RESULTS

The DIC results can be divided into two main areas connected to different stop criteria: (1) Crack detection, (2) Crack width monitoring with and without the described correction for out-of-plane movement. Data treatment is performed using a commercial software (GOM, 2018).

3.1 Crack detection

Initial crack formation- and related influence on the beam response is detected in three ways: (1) using DIC strain concentrations, (2) by close visual inspection in the DIC photos from the test, and (3) by stiffness change detection in the moment/deflection curves. In addition to these three elements, the expected cracking moment has also been estimated. In this estimation, it proved valuable to work with the CFRP post-tensioning system, where the cracking load was primarily dependent on the post-tensioning level. The initial crack detection results are seen in Table 1.

In general, the results show that the expected value for the cracking moment and the stiffness change observations from the curves match well. An increase of the post-tensioning level results in a higher moment magnitude before crack initiation occurs. In all cases, DIC detection of initial

cracking occurs prior to visual detection and in most cases, the DIC method reveals crack formation prior to any other detections. The low DIC moment values for ANSMR50-1 and ANSMR50-2 are dedicated to a partly pre-cracked cross section, which results in a low contribution from the concrete. It is interesting that this is only observed by DIC and not by stiffness change, which indicates that DIC crack detection might not be directly associated with global structural behavior (stiffness change).

Table 1. Bending moment for which cracks were detected by DIC (“DIC”), visual inspection of the photos (“Visual”), and based on the change of stiffness in the moment-deflection curve (“Stiffness change”).

Beam	DIC [kNm]		Visual [kNm]		Stiffness change [kNm]	Expected cracking moment [kNm]
	Side	Bottom	Side	Bottom		
*Ref-NSMR1	11.8	12.4	61.1	58.3	16	17
Ref-NSMR2	6.7	7.8	59.9	29.3	16	17
**ANSMR50-1	9.9	12.2	27.2	59.6	35	37
ANSMR50-2	22.5	18.2	63.0	68.4	35	37
ANSMR50-3	35.7	41.4	70.4	61.7	35	37
ANSMR70- 1	37.2	37.2	64.4	52.8	48	46
ANSMR70- 2	46.3	43.1	65.5	88.7	48	46

* Ref-NSMR (reference beams strengthened with NSMR CFRP and no post-tensioning), ** ANSMR (Anchored near surface mounted reinforcement).

Visual detection is performed by close study of the photos used in the DIC analysis. For all cases but one, the detection occur after observation of a significant stiffness change.

Post-tensioning levels have shown to significantly influence the crack formation during loading. For beams without post-tensioning, the cracks slowly form beginning with vague indications of a crack to a developed crack. For beams with post-tensioning, the cracks form almost from one photo to another (frame rate 0.1f/s). This is illustrated in

Figure 3, for no post-tensioning (Ref-NSMR1) and 70% post-tensioning (ANSMR70-2).

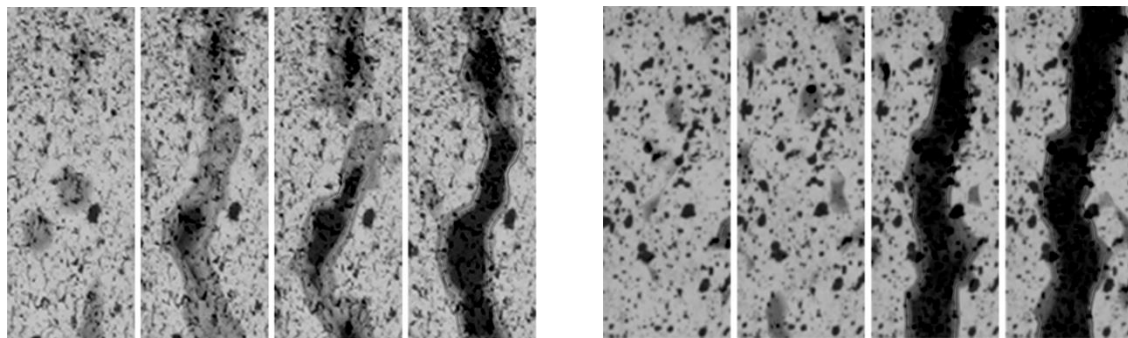


Figure 3. Crack formation. Left: No post-tensioning, Right: 70% post-tensioning. Frame rate 0.1f/s.

3.2 Crack width

After detection of a crack, crack widths can be monitored throughout the test. This is easiest done with the camera from the side of the beam, because very limited out-of-plane movement occurs. However, for full-scale slab bridge tests, it is only possible to monitor the bottom surface.

Upon detection, the cracks are usually of insignificant size and well below any stop criterion. In the proposal for stop criteria by Lantsoght et al (2018) the threshold for bending cracks is set to $w_{max} \leq 0.5$ mm, based on the German guideline, DAfStb (2000). In Eurocode 2, the maximum allowable crack width for service limit loads for concrete members in buildings is set to $w_{max} \leq 0.3$ mm for reinforced members and pre-stressed members with unbonded tendons and to $w_{max} \leq$

0.2 mm for pre-stressed members with bonded tendons, European Committee for Standardization (2008). These threshold values form the basis for this study. With regard to the Eurocode, the two beams without post-tensioning are set to comply with the demand of $w_{max} \leq 0.3$ mm.

The points for which the thresholds are met, using the side images only, are plotted in Figure 4 in the loading regime. Crack detection occurs early in the loading regime and the crack growth can be closely monitored and observed for crack width stop criteria. The Eurocode thresholds are met at approximately 50% of the linear elastic cracked regime, whereas the recommendation for bridge slab tests are met near the yielding point of the steel rebars. Further assessment of the safety in this is not analyzed, but it is noted that it is possible to monitor crack width development at significantly lower magnitudes than the crack width thresholds.

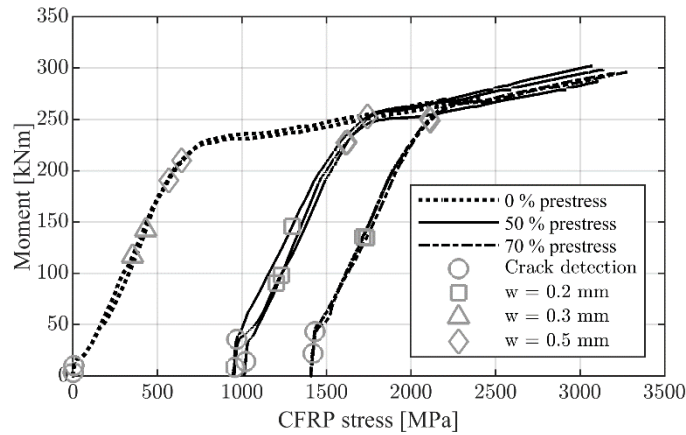


Figure 4. Loading regime and flexural crack widths for the side images only.

As previously described, the crack widths measured underneath the beams have to be corrected. The camera distance in the tests was $h = 242$ mm. Such a relatively short distance can create a large pseudo strain from just a few millimeters of out-of-plane movement. Measured values of crack width at the Eurocode thresholds for three different beams and post-tensioning levels are shown in Figure 5. The measured crack width, L_x , is much larger for the bottom camera before correction. The first component of the geometric correction, ε_{oop} , is dependent on the camera distance, h , and the surface deflection, n (see Equation 1). Surface deflection was measured using the DIC images from the side camera (dY in the plots in Figure 5). The rotation of the surface at this point is of insignificant size and therefore the rotational correction is neglected. To obtain the true crack width, the strain correction has to be multiplied by the length of the 2-point distance on the reference image, L , and subtracted from the measured crack width, L_x (Equation 2).

$$\varepsilon_{oop} = \frac{h}{h - n} - 1 \quad (1)$$

$$w_{true} = L_x - \varepsilon_{oop} \cdot L \quad (2)$$

The corrected values resemble the values measured on the side. For the beam without post-tensioning, the value is 3.6 % lower and for the two post-tensioned beams the value is approximately 20 % lower. It has to be noted that the pictures are shot from two different camera angles, with similar but different cameras, and that the crack development/crack width is not necessarily the exact same in the two locations. In addition, the correction was observed to be sensitive to small changes in deflection and ruler positioning. The ruler was placed exactly at the edge of the observed crack dispersion area and when done meticulously and consistently, the results seemed to fit well for the tests. Following this correction approach, it thereby seems possible to monitor crack widths using 2D DIC from underneath a structure.

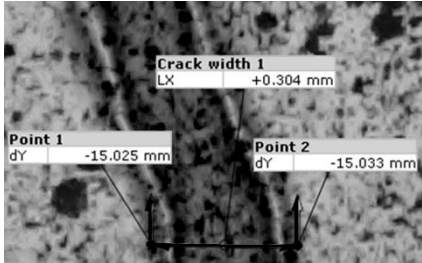
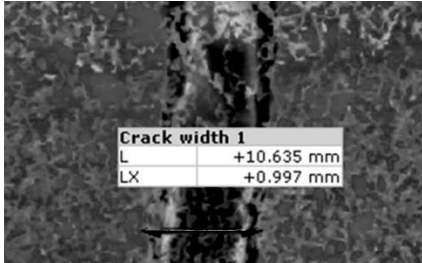
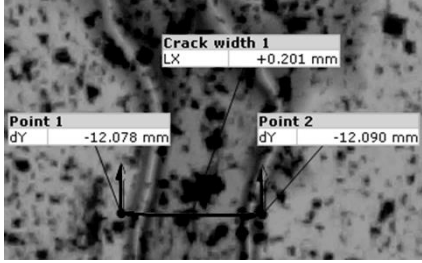
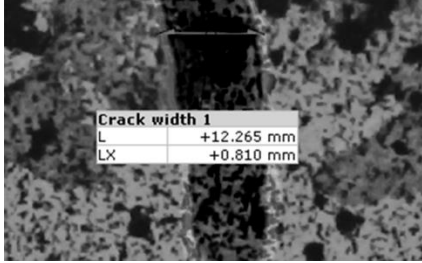
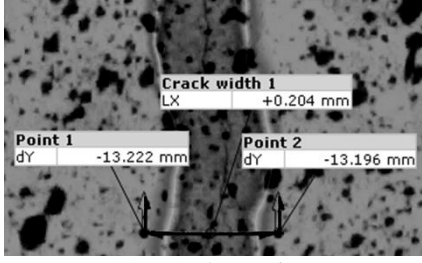
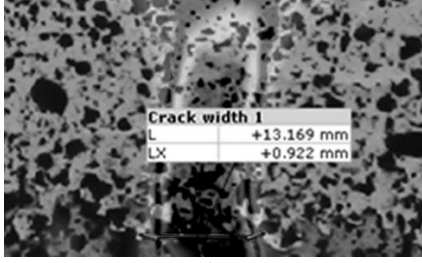
 <p>Crack width 1 LX +0.304 mm</p> <p>Point 1 dY -15.025 mm</p> <p>Point 2 dY -15.033 mm</p> <p><i>Ref-NSMRI (0%) – Side.</i></p>	 <p>Crack width 1 L +10.635 mm LX +0.997 mm</p> <p><i>Ref-NSMRI (0%) – Bottom.</i></p>	<p>Side photo: $n = 15.029 \text{ mm}$ $w = 0.304 \text{ mm}$</p> <p>Bottom photo: $L = 10.635 \text{ mm}$ $L_x = 0.997 \text{ mm}$ → $w_{true} = 0.293 \text{ mm}$</p>
 <p>Crack width 1 LX +0.201 mm</p> <p>Point 1 dY -12.078 mm</p> <p>Point 2 dY -12.090 mm</p> <p><i>ANSMR50-2 (50%) – Side.</i></p>	 <p>Crack width 1 L +12.265 mm LX +0.810 mm</p> <p><i>ANSMR50-2 (50%) – Bottom.</i></p>	<p>Side photo: $n = 12.084 \text{ mm}$ $w = 0.201 \text{ mm}$</p> <p>Bottom photo: $L = 12.265 \text{ mm}$ $L_x = 0.810 \text{ mm}$ → $w_{true} = 0.165 \text{ mm}$</p>
 <p>Crack width 1 LX +0.204 mm</p> <p>Point 1 dY -13.222 mm</p> <p>Point 2 dY -13.196 mm</p> <p><i>ANSMR70-2 (70%) – Side.</i></p>	 <p>Crack width 1 L +13.169 mm LX +0.922 mm</p> <p><i>ANSMR50-2 (70%) – Bottom.</i></p>	<p>Side photo: $n = 13.209 \text{ mm}$ $w = 0.204 \text{ mm}$</p> <p>Bottom photo: $L = 13.169 \text{ mm}$ $L_x = 0.922 \text{ mm}$ → $w_{true} = 0.161 \text{ mm}$</p>

Figure 5. Comparison of crack widths before and after correction.

4 CONCLUSION

2D DIC was evaluated in relation to proof load testing of concrete slab bridges, where crack monitoring can only be done from underneath. Its applicability was investigated with regard to (1) time of crack detection compared to visual detection, (2) time of crack detection compared to time of reaching crack width threshold values, and (3) crack width evaluation using 2D-DIC strain correction for out-of-plane deflection. The results show that cracks seem to be detectable by DIC prior to both visual detection and any significant stiffness change. This is a major benefit in proof load testing but also shows that DIC crack detection cannot be directly linked to global stiffness change. After crack detection, it seems possible to follow crack development throughout the test with a precision that enables a threshold comparison with stop criteria for the crack width. Crack widths can be corrected for pseudo deformation caused by out-of-plane movement using the developed geometric correction method. The method showed sensitivity to placing of the crack width 2-point distance, but when placed consistently at the edge of the crack dispersion area, the values seemed to fit well. It is hypothesized that the approach holds great potential in crack monitoring of full-scale slab bridge tests and thus for the application as stop criteria.

ACKNOWLEDGEMENTS

A sincere gratitude is addressed to S&P Denmark, the Danish road directorate, Jorcks foundation and Perstrup Beton Industri A/S for the contributions to the ongoing research. Furthermore, the

work of former students Klavs Foged Skovby and Nicolaj Jacob Birkebæk Thomsen, and assistance of the technical staff at the DTU CasMat laboratory facility, are greatly acknowledged.

REFERENCES

- AASHTO, 2011, *The manual for bridge evaluation*. 2nd edn. Washington, D.C.: American Association of State Highway and Transportation Officials.
- ACI Committee 437, 2013, *Code Requirements for Load Testing of Existing Concrete Structures (ACI 437.2M-13)*. Farmington Hills, MA.
- DAfStb, 2000, *DAfStb-Guideline: Load Tests on Concrete Structures*. Berlin, Germany: Deutscher Ausschuss für Stahlbeton.
- Elmont, V. J., 1913, 'Test-loading until breaking point of a 100-foot arch bridge', *Canadian Engineer*.
- European Committee for Standardization, 2008, 'Eurocode 2: Design of concrete structures - Part 1: General rules and rules for buildings'.
- GOM, 2018, 'GOM Correlate Professional'.
- Goodpasture, D. W. and Burdette, E. G., 1973, 'Full Scale Tests to Failure of Four Highway Bridges', *American Railway Engineering Association*, 74(643), pp. 454–473.
- Halding, P. S., Schmidt, J. W., Jensen, T. W. and Henriksen, A.H., 2017, 'Structural response of full-scale concrete bridges subjected to high load magnitudes', in *SMAR*, Zürich, Switzerland.
- Halding, P. S., Schmidt, J. W. and Christensen, C. O., 2018a, 'DIC-monitoring of full-scale concrete bridge using high-resolution wide-angle lens camera', in *9th International Conference on Bridge Maintenance, Safety and Management*, Melbourne, Australia, pp. 1492–1499.
- Halding, P. S., Christensen, C. O. and Schmidt, J. W., 2018b, 'Surface Rotation Correction and Strain Precision of Wide-Angle 2D DIC for Field Use', *Journal of Bridge Engineering*.
- ICE, 1998, *Guidelines for the Supplementary Load Testing of Bridges*. London, England: The Institution of Civil Engineers - National Steering Committee for the Load Testing of Bridges.
- Lantsoght, E., Yang, Y., Tersteeg, R., van der Veen, C., de Boer, A. and Hordijk, D. A., 2016, 'Stop criteria for proof loading', *Life-Cycle of Engineering Systems: Emphasis on Sustainable Civil Infrastructure*.
- Lantsoght, E., Yang, Y., van der Veen, C. and de Boer, A., 2016, 'Ruytenschildt Bridge: Field and laboratory testing', *Engineering Structures*. doi: 10.1016/j.engstruct.2016.09.029.
- Lantsoght, E., van der Veen, C., Hordijk, D. A. and de Boer, A., 2017, 'Development of recommendations for proof load testing of reinforced concrete slab bridges', *Engineering Structures*. Elsevier Ltd, 152, pp. 202–210. doi: 10.1016/j.engstruct.2017.09.018.
- Lantsoght, E., Yang, Y., van der Veen, C., Hordijk, D. A. and de Boer, A., 2018, 'Stop criteria for proof load tests verified with field and laboratory testing of the Ruytenschildt Bridge Ruytenschildt field test', in *IABSE Conference*, Kgs. Lyngby, Denmark, pp. 1–8.
- NRA, 2014, *Load Testing for Bridge Assessment*. Dublin, Ireland: NRA.
- Omondi, B., Aggelis, D. G., Sol, H. and Sitters, C., 2016, 'Improved crack monitoring in structural concrete by combined acoustic emission and digital image correlation techniques', *Structural Health Monitoring: An International Journal*, 15(3), pp. 359–378. doi: 10.1177/1475921716636806.
- Rösli, A., 1963, 'Die Versuche an der Glatzbrücke in Opfikon', *Eidgenössische Materialprüfungs- Und Versuchsanstalt Für Industrie, Bauwesen Und Gewerbe*, 192(85).
- Schmidt, J. W., Hansen, S. G., Barbosa, R. A. and Henriksen, A., 2014, 'Novel shear capacity testing of ASR damaged full scale concrete bridge', *Engineering Structures*. doi: 10.1016/j.engstruct.2014.08.027.
- Schmidt, J. W., Halding, P. S., Jensen, T. W. and Engelund, S., 2018, 'High Magnitude Loading of Concrete Bridges', *ACI Special Publication 323, ACI SP 323 Evaluation of Concrete Bridge Behavior through Load Testing - International Perspectives*, p. 9.1-9.20.
- Vejdirektoratet, 2004, 'Pålidelighedsbaseret klassifisering af eksisterende broers bæreevne'.
- Zhang, J., Peng, H. and Cai, C. S., 2011, 'Field Study of Overload Behavior of an Existing Reinforced Concrete Bridge under Simulated Vehicle Loads', *Journal of Bridge Engineering*, 16(2), pp. 226–237. doi: 10.1061/(asce)be.1943-5592.0000140.
- Zhang, J., Peng, H. and Cai, C. S., 2013, 'Destructive Testing of a Decommissioned Reinforced Concrete Bridge', *Journal of Bridge Engineering*, 18(6), pp. 564–569. doi: 10.1061/(asce)be.1943-5592.0000408.